CHEMICAL ENGINEERING TRANSACTIONS
VOL. 109, 2024
A publication of AIDIC
The Italian Association of Chemical Engineering
Online at www.cetjournal.it
Guest Editors: Leonardo Tognotti, Rubens Maciel Filho, Viatcheslav Kafarov
Copyright © 2024, AIDIC Servizi S.r.l.
ISBN 979-12-81206-09-0; **ISSN** 2283-9216
DOI: 10.3303/CET24109103

Investigating Mixed Refrigerant Solidification in Hydrogen Liquefaction Processes

Federica Restelli*, Laura A. Pellegrini

GASP - Group on Advanced Separation Processes & GAS Processing, Dipartimento di Chimica, Materiali e Ingegneria Chimica "G. Natta", Politecnico di Milano, Piazza Leonardo da Vinci 32, 20133 Milano, Italy
federica.restelli@polimi.it

Within hydrogen liquefaction cycles, refrigerant mixtures reach highly critical conditions, with temperatures approaching the solidification temperatures of the pure components. To ensure the feasibility of the hydrogen liquefaction process, it is necessary to verify that such mixtures do not solidify under specified temperature and pressure conditions. This verification is carried out through the minimization of Gibbs free energy by simulating a RGibbs reactor in Aspen Plus® V11. For a given refrigerant mixture, comprising light hydrocarbons, hydrogen and nitrogen, the solidification temperature is determined as a function of pressure. The solidification curve is plotted for four mixed refrigerants that have been utilized in the literature for the precooling section of the hydrogen liquefaction process. The composition of the mixed refrigerant greatly affects the minimum temperature at which a refrigerant can be safely used without incurring solid precipitation, which varies between 60 K and 100 K. This work provides a guide for selecting the appropriate mixed refrigerant composition and operating conditions, with the aim to enhance the efficiency, reliability, and safety of hydrogen liquefaction technologies.

1. Introduction

The liquefaction of hydrogen is a crucial step for its efficient storage and transportation on a large-scale (Restelli et al., 2024). Numerous process configurations have been investigated in the literature. The built hydrogen liquefaction plants are all based on a liquid N_2-precooled Claude cycle (Restelli et al., 2023b). However, specific electricity consumptions (SEC) for these plants are higher than 10 kWh/kg. Therefore, researchers are studying more efficient configurations for this process, also in view of its application on a large scale. In 2002, Quack proposed a liquefaction plant involving Joule-Brayton (J-B) refrigeration cycles using a mixture of ethane and propane for precooling and of helium and neon for cryogenic cooling, achieving a SEC of 6.98 kWh/kg. Shimko and Gardiner (2008) developed a liquefaction cycle precooled by helium with SEC of 8.73 kWh/kg. Valenti and Macchi (2008) proposed a conceptual liquefier based on four cascaded helium J-B cycles, that presents a SEC of 5.04 kWh/kg, but also a high investment cost due to the large number of compression stages. Krasae-in (2014) proposed a liquefaction process with a J-B precooling cycle using a mixed refrigerant (MR) made of methane, ethane, n-butane, nitrogen and hydrogen. The cryogenic cooling section involves four cascaded J-B cycles in which hydrogen is used as a refrigerant. The SEC of the proposed plant is 5.35 kWh/kg. In 2013, the conclusion of the European project IDEAHLY (Stolzenburg et al., 2013) set a target for subsequently developed processes of a specific electricity consumption of 6 kWh/kg. The process involves precooling with a mixture of refrigerants, such as nitrogen, methane, ethane, propane and n-butane, and cooling with a mixture called Nelium (75 mol% helium and 25 mol% neon). A MR precooled dual-pressure H_2 Claude cycle and a MR cascade cycle were simulated by Cardella et al. (2017). The composition of the precooling mixed refrigerant, which flows in a Joule-Thomson cycle, is optimized subject to a constraint of a maximum of four components, including nitrogen and light hydrocarbons. Sadaghiani and Mehrpooya (2017) proposed a MR cascade liquefaction process in which the precooling mixed refrigerant comprises nine refrigerant components. The stated performance in terms of SEC is 4.41 kWh/kg. The process proposed by Kuendig et al. (2006) is based on a Claude cycle with precooling by liquefied natural gas (LNG) and nitrogen. The low SEC of 4 kWh/kg is achieved through process integration, subjected to the presence of an LNG regasification plant at the hydrogen liquefaction site. Qyyum

Paper Received: 05 February 2024 ; Revised: 25 February 2024 ; Accepted: 21 March 2024
Please cite this article as: Restelli F., Pellegrini L., 2024, Investigating Mixed Refrigerant Solidification in Hydrogen Liquefaction Processes, Chemical Engineering Transactions, 109, 613-618 DOI:10.3303/CET24109103

et al. (2021) proposed a process operating with three cascading J-B cycles using refrigerant mixtures as working fluids. The stated performance in terms of SEC is 6.45 kWh/kg.
Among the numerous techniques employed for hydrogen liquefaction, mixed refrigerant precooling stands out as a prominent method due to its higher efficiency. In fact, to minimize exergy destruction, it is necessary to obtain a close match between the hot and cold composite curves of the heat exchangers. To achieve this goal, mixed refrigerants are preferred to pure substances since mixtures' phase change occurs at variable temperature, while pure substances evaporate at constant temperature. The use of pure refrigerants offers the advantage of simpler design and, hence, lower investment costs. However, as project scale increases, it becomes more important to obtain lower operating costs, which are related to SEC and ultimately to exergy efficiency. The MR technique is extensively employed in today's LNG sector owing to its comparatively modest energy usage and minimal equipment requirements (Restelli et al., 2023a). However, the implementation of MR cycles in hydrogen liquefaction processes is more challenging than in natural gas liquefaction processes due to the significantly lower temperature required for liquefying hydrogen (20 K) compared to natural gas (112 K). At such low temperatures the solidification of refrigerants is an issue that must be taken into account during the design of the liquefaction process. Solidification not only disrupts the smooth operation of the liquefaction system but also poses safety concerns. Successful implementation of MR precooling cycle in hydrogen liquefaction plants relies heavily on the appropriate selection of refrigerants and operating conditions (temperature T and pressure P) at which they are utilized. In this work, the solidification of mixed refrigerants in hydrogen liquefaction processes is investigated by adopting the Gibbs free energy minimization approach to determine the stable phases present at equilibrium under specified temperature and pressure conditions for a given mixed refrigerant. While previous literature has focused on the optimization of MR composition, the novelty of this work lies in providing a method to identify the temperature over which such mixed refrigerants can be safely utilized.

2. Methodology

The Gibbs free energy minimization approach is a fundamental principle in thermodynamics used to determine the stable phases present at equilibrium in a mixture under given temperature and pressure conditions. It relies on the fact that, at equilibrium, the Gibbs free energy of the system is minimized with respect to changes in composition and phase. Once the stable phases are determined, phase equilibrium calculations can be performed to predict the composition of each phase and their respective amounts in the mixture.
In this work, the minimization of the Gibbs free energy of the system is carried out by simulating an RGibbs reactor in Aspen Plus® V11 (AspenTech, 2016). The reactor in Figure 1 receives a given refrigerant mixture as input (IN) and outputs the phases, vapor (V), liquid (L), and solid (S), present at equilibrium under the specified pressure and temperature conditions. The underlying assumptions made during the simulation are the homogeneity of the mixture, the achievement of thermal equilibrium conditions and the eutectic behavior of the system (i.e. no solid solution is present). The species considered as refrigerants are: CH_4, C_2H_6, C_3H_8, n-C_4H_{10}, i-C_4H_{10}, n-C_5H_{12}, CF_4 (known as R14), C_2H_4, N_2, and H_2.

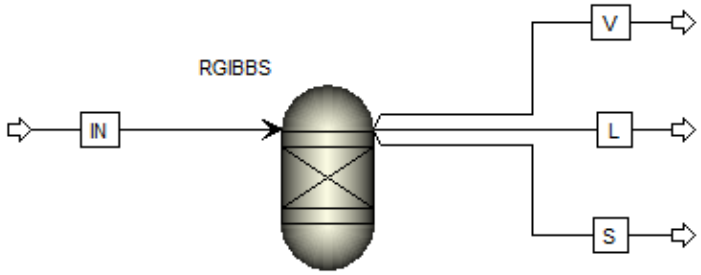

Figure 1: RGibbs reactor simulation in Aspen Plus® V11.

The simulation of this unit requires knowledge of the values of the standard enthalpy and Gibbs free energy of formation in the solid phase, $\Delta H^0_{f,S}$ and $\Delta G^0_{f,S}$, respectively, for each compound that is expected to potentially precipitate under the specified temperature and pressure conditions. The values of these quantities for the considered species are not reported in the literature. Therefore, it is necessary to estimate them from known thermodynamic properties. The calculation is performed using the scheme shown in Figure 2.

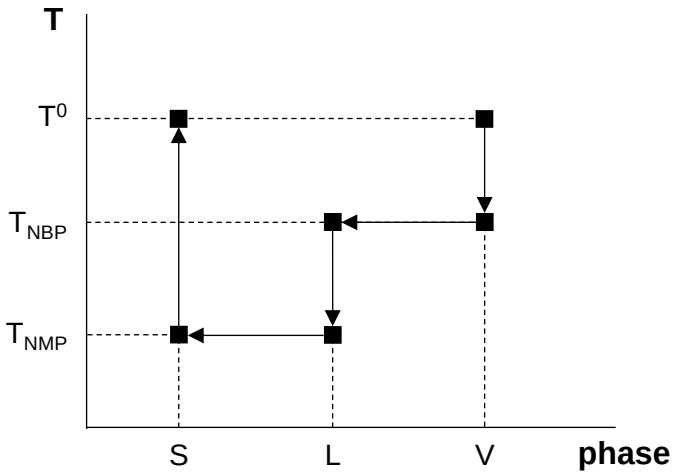

Figure 2: Scheme for calculating standard enthalpy, entropy, and Gibbs free energy of formation in the solid phase.

The standard enthalpy of formation in the solid phase is calculated starting from the standard enthalpy of formation in the vapor phase, $\Delta H^0_{f,V}$, to which the following contributions must be added, as in Eq(1):

- the enthalpy change at P^0 (1 bar) from the vapor state at T^0 (298.15 K) to the saturated vapor state, which is at the normal boiling point temperature T_{NBP},
- the opposite of the enthalpy of vaporization at T_{NBP}, $-\Delta H_{ev}@T_{NBP}$,
- the enthalpy change at P^0 from the saturated liquid state to the liquid state at the incipient solidification point, which is at the normal melting point temperature T_{NMP},
- the opposite of the enthalpy of melting at T_{NMP}, $-\Delta H_{melt}@T_{NMP}$,
- the enthalpy change at P^0 from the solid state at T_{NMP} to the solid state at T^0.

$$\Delta H^0_{f,S} = \Delta H^0_{f,V} + \int_{T^0}^{T_{NBP}} c_P dT - \Delta H_{ev} @ T_{NBP} + \int_{T_{NBP}}^{T_{NMP}} c_L dT - \Delta H_{melt} @ T_{NMP} + \int_{T_{NMP}}^{T^0} c_S dT \quad (1)$$

In Eq(1), c_P, c_L and c_S stand for the vapor specific heat capacity at constant pressure, liquid specific heat capacity and solid specific heat capacity, respectively. They are functions of T.
The standard entropy of formation in the solid phase is calculated starting from the standard entropy of formation in the vapor phase, $\Delta S^0_{f,V}$, to which the following has been added, as in Eq(2):

- the entropy change at P^0 from the vapor state at T^0 to the saturated vapor state, which is at T_{NBP},
- the opposite of the entropy of vaporization at T_{NBP}, $-\Delta H_{ev}@T_{NBP} / T_{NBP}$,
- the entropy change at P^0 from the saturated liquid state to the liquid state at the incipient solidification point, which is at T_{NMP},
- the opposite of the entropy of melting at T_{NMP}, $-\Delta H_{melt}@T_{NMP} / T_{NMP}$,
- the entropy change at P^0 from the solid state at T_{NMP} to the solid state at T^0.

$$\Delta S^0_{f,S} = \Delta S^0_{f,G} + \int_{T^0}^{T_{NBP}} \frac{c_P}{T} dT - \frac{\Delta H_{ev} @ T_{NBP}}{T_{NBP}} + \int_{T_{NBP}}^{T_{NMP}} \frac{c_L}{T} dT - \frac{\Delta H_{melt} @ T_{NMP}}{T_{NMP}} + \int_{T_{NMP}}^{T^0} \frac{c_S}{T} dT \quad (2)$$

Finally, the standard Gibbs free energy of formation in the solid phase is calculated with equation (3).

$$\Delta G^0_{f,S} = \Delta H^0_{f,S} - T^0 \Delta S^0_{f,S} \quad (3)$$

Table 1 shows the results obtained with Eq(1) and Eq(3) for the considered species.
The Peng Robinson Equation of State is selected to compute the volumetric properties of the vapor and liquid phases. The other parameters required in the calculations, such as the correlations for the heat capacities and solid molar volume are taken from the Aspen databank.

Table 1: $\Delta H^0_{f,S}$ and $\Delta G^0_{f,S}$ for the considered species.

Species	$\Delta H^0_{f,S}$ (kJ/mol)	$\Delta G^0_{f,S}$ (kJ/mol)
CH_4	-75.183	-37.828
C_2H_6	-85.683	-21.240
C_3H_8	-123.440	-8.189
n-C_4H_{10}	-150.300	-8.606
i-C_4H_{10}	-145.902	-14.200
n-C_5H_{12}	-152.406	0.244
R14	-909.604	-886.362
C_2H_4	78.730	69.370
N_2	9.885	9.816
H_2	-6.626	26.356

Four case studies are examined, having the following MR compositions, taken from the literature:

- MR1: 0.30 CH_4, 0.31 C_2H_6, 0.25 i-C_4H_{10} and 0.14 N_2 (Cardella et al., 2017),
- MR2: 0.24 CH_4, 0.28 C_2H_6, 0.26 n-C_4H_{10}, 0.18 N_2 and 0.04 H_2 (Krasae-in, 2014),
- MR3: 0.17 CH_4, 0.07 C_2H_6, 0.18 C_3H_8, 0.02 n-C_4H_{10}, 0.15 n-C_5H_{12}, 0.16 N_2, 0.08 CF_4, 0.16 C_2H_4 and 0.04 H_2 (Sadaghiani and Mehrpooya, 2017),
- MR4: 0.034 CH_4, 0.109 C_2H_6, 0.768 C_3H_8, 0.044 N_2 and 0.045 H_2 (Qyyum et al., 2021).

These mixtures have been optimized by the cited authors to maximize the exergy efficiency, hence minimizing the SEC, of the proposed processes.

3. Results and discussion

Solidification curves are determined for precooling mixtures adopted in the works by Cardella et al. (2017), Krasae-in (2014), Sadaghiani and Mehrpooya (2017), and Qyyum et al. (2021). The results are reported in Figure 3.

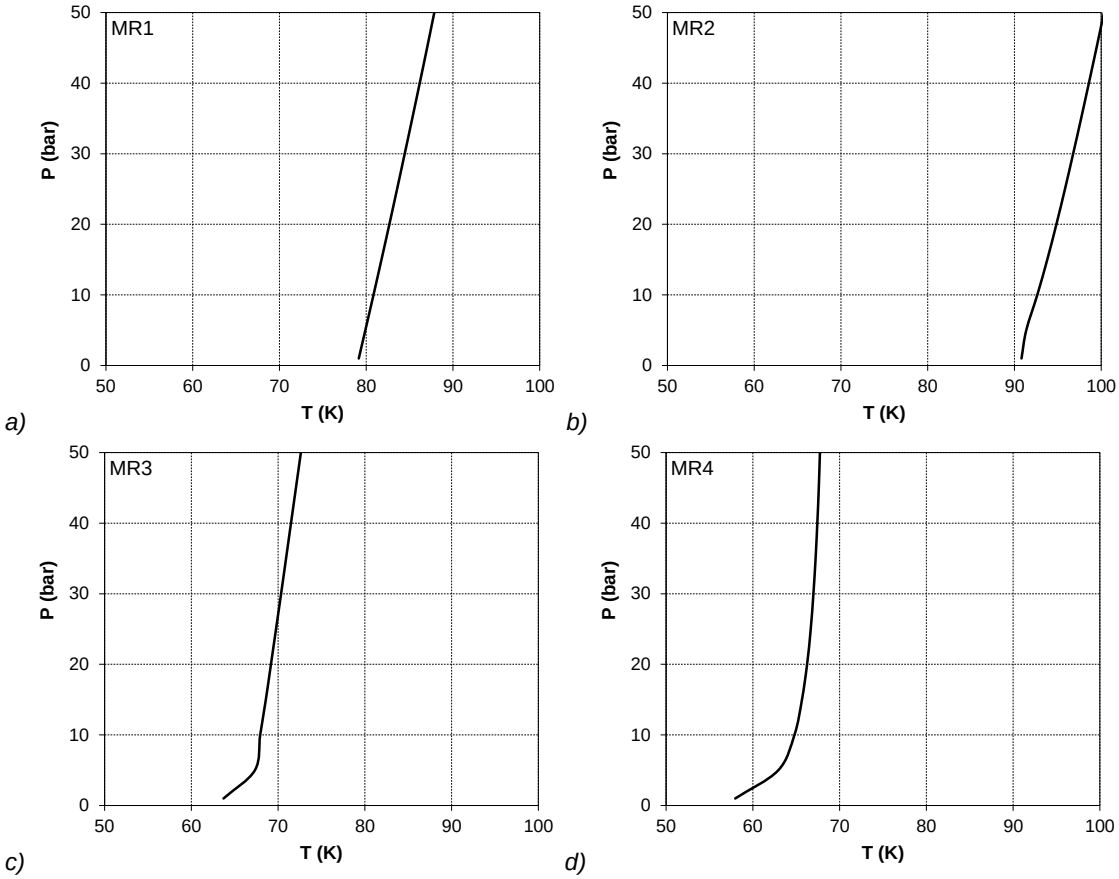

Figure 3: Solidification curve of the considered precooling mixed refrigerant: a) MR1, b) MR2, c) MR3, and d) MR4.

From Figure 3 it is possible to notice that MR1 must be utilized at temperatures higher than 80-90 K (depending on the operating pressure) to prevent solid precipitation, whereas MR2 solidifies below 90 K, even at atmospheric pressure. This difference is attributed to the presence of n-butane in MR2, which has a normal melting point temperature of 134.9 K, compared to i-butane in MR1, with a T_{NMP} of 113.7 K, making MR2 more prone to solidification. Refrigerant mixtures MR3 and MR4 can be used to cool the process to approximately 70 K without incurring solidification. They both contain propane, which has the lowest normal melting point temperature among alkanes, 85.5 K. It is important to notice that MR2 and MR4 consist of 5 components and MR3 comprises 9 components. The presence of numerous species in refrigeration mixtures poses a challenge in managing refrigerant makeup in response to leakages. It becomes imperative to continuously monitor the composition and conduct calculations to determine the nature and extent of compounds required for makeup, ensuring that the composition remains consistent with the design specifications. Another issue associated with MR3 is the presence of R14, which is considered harmful for the environment, having a global warming potential of 5700 (where 1 is that of CO_2).
One possible strategy to reduce the operating temperature of the mixed refrigerants involves cooling the mixture by letting it flow at the hot side of the heat exchangers until a condition of liquid-vapor equilibrium is established. After phase separation, the vapor, containing predominantly lower boiling components, undergoes further precooling before being expanded and used to remove heat at the cold side of the exchangers. While the liquid, rich in higher boiling components, susceptible to solidification at lower temperatures, is expanded and used for the initial precooling.
It is worth noting that in this context the solidification temperature refers to the solid-fluid equilibrium temperature. In practice, a process can be operated just below this equilibrium temperature (with a very small degree of subcooling) without observing the formation of solids, even though these solids are thermodynamically stable (Sampson et al., 2022). This is because the nucleation induction time (the time it takes for solids to form) is significantly longer than the residence time of fluid in the process equipment. Probabilistic models relying on experimental data on solid formation would provide a more accurate prediction of solid precipitation under specific operating conditions. However, such data are not available for the mixtures under consideration.
The results obtained provide an indication of the minimum temperature that can be reached by the precooling MR without incurring solid formation. This information is crucial for the safe design of the precooling refrigeration cycle in hydrogen liquefaction plants.

4. Conclusions

The results of this study provide an interesting connection between theory and practical application. Predictions are made regarding the lowest temperatures achievable with a given combination of species, without the formation of solids. Researchers must consider the minimum operating temperature of refrigerant mixtures when designing the hydrogen liquefaction process. While utilizing optimization algorithms for minimizing the specific electricity consumption of the liquefaction process, attention must be paid to the choice of the range within which the minimum temperature of the precooling cycle varies. The solidification of the precooling MR components must be taken into account by imposing the value of the lower temperature bound higher than the solidification temperature. An interesting future development of this work would involve experimental testing to validate these predictions. One possible technique involves preparing a specific mixture and loading it into a pressure cell equipped with a window to visualize the formation of solids. The experiments proceed with temperature ramping down and up, observing the solidification and melting phenomena, and annotating the pressure and temperature at which they occur.

Nomenclature

c_L – liquid molar specific heat capacity, kJ/(mol·K)
c_P – vapor molar specific heat capacity at constant pressure, kJ/(mol·K)
c_S – solid molar specific heat capacity, kJ/(mol·K)
$\Delta G^0_{f,V}$ – vapor standard Gibbs free energy of formation, kJ/mol
$\Delta G^0_{f,S}$ – solid standard Gibbs free energy of formation, kJ/mol
$\Delta H^0_{f,V}$ – vapor standard enthalpy of formation, kJ/mol
$\Delta H^0_{f,S}$ – solid standard enthalpy of formation, kJ/mol
$\Delta H_{ev}@T_{NBP}$ – enthalpy of vaporization, kJ/mol
$\Delta H_{melt}@T_{NMP}$ – enthalpy of vaporization, kJ/mol
$\Delta S^0_{f,V}$ – vapor standard entropy of formation, kJ/(mol·K)
$\Delta S^0_{f,S}$ – solid standard entropy of formation, kJ/(mol·K)
P – pressure, bar
P^0 – standard pressure, bar
T – temperature, K
T^0 – standard temperature, K
T_{NBP} – normal boiling point temperature, K
T_{NMP} – normal melting point temperature, K

References

AspenTech, 2016, Aspen Plus®, Burlington (MA), United States.

Cardella U., Decker L., Sundberg J., Klein H., 2017, Process optimization for large-scale hydrogen liquefaction, International Journal of Hydrogen Energy, 42, 12339–12354.

Krasae-In S., 2014, Optimal operation of a large-scale liquid hydrogen plant utilizing mixed fluid refrigeration system, International Journal of Hydrogen Energy, 39, 7015–7029.

Kuendig. A., Loehlein K., Kramer G.J., Huijsmans J., 2006, Proceedings of the 16th world hydrogen energy conference, 3326–3333.

Qyyum M.A., Riaz A., Naquash A., Haider J., Qadeer K., Nawaz A., Lee H., Lee M., 2021, 100% saturated liquid hydrogen production: Mixed-refrigerant cascaded process with two-stage ortho-to-para hydrogen conversion, Energy Conversion and Management, 246, 114659.

Quack H., 2002, Conceptual design of a high efficiency large capacity hydrogen liquefier, AIP Conference Proceedings, 613, 255.

Restelli F., Gambardella M., Pellegrini L.A., 2023a, Green vs fossil-based energy vectors: A comparative techno-economic analysis of green ammonia and LNG value chains, Journal of Environmental Chemical Engineering, 12(1), 111723.

Restelli F., Spatolisano E., Pellegrini L.A., 2023b, Hydrogen Liquefaction: a Systematic Approach to its Thermodynamic Modeling, Chemical Engineering Transactions, 99, 433–438.

Restelli F., Spatolisano E., Pellegrini L.A., Cattaneo S., de Angelis A.R., Lainati A., Roccaro E., 2024, Liquefied hydrogen value chain: A detailed techno-economic evaluation for its application in the industrial and mobility sectors, International Journal of Hydrogen Energy, 52, 454–466.

Sadaghiani M.S., Mehrpooya M., 2017, Introducing and energy analysis of a novel cryogenic hydrogen liquefaction process configuration, International Journal of Hydrogen Energy, 42, 6033–6050.

Sampson C.C., Metaxas P.J., Barwood M.T.J., Sinclair-Adamson R., Falloon P.E., Stanwix P.L., Johns M.L., May E.F., 2022, Experimental solid–liquid equilibria and solid formation kinetics for carbon dioxide in methane for LNG processing, AIChE Journal, 69(4), e18001.

Shimko M.A., Gardiner M.R., 2008, FY 2008 Annual Progress Report, DOE Hydrogen Program.

Stolzenburg K., Berstad D., Decker L., Elliott A., Haberstroh C., Hatto C., Klaus M., Mortimer N.D., Mubbala R., Mwabonje O., Nekså P., Quack H., Rix J.H.R., Seemann I., Walnum H.T., 2013, Efficient liquefaction of hydrogen: Results of the IDEALHY project, XX energie – symposium, Stralsund, Germany, 7 - 9 November 2013.

Valenti G., Macchi E., 2008, Proposal of an innovative, high-efficiency, large-scale hydrogen liquefier, International Journal of Hydrogen Energy, 33, 3116–3121.